Virologica Sinica 38 (2023) 699–708

Contents lists available at ScienceDirect

Virologica Sinica

journal homepage: www.keaipublishing.com/en/journals/virologica-sinica
www.virosin.org

Research Article

Long noncoding RNA 1392 regulates MDA5 by interaction with ELAVL1 to inhibit coxsackievirus B5 infection

Jing Li, Jinwei Li, Peiying Teng, Fan Yang, Jihong Zhang, Bo Sun, Wei Chen *

Medical School, Kunming University of Science and Technology, Kunming, 650500, China

ARTICLE INFO

Keywords:
Long noncoding RNAs (lncRNAs)
Coxsackievirus B5 (CVB5)
Type I interferon (IFN-I) signaling pathway
Melanoma differentiation-associated gene 5 (MDA5)
ELAV like RNA binding protein 1 (ELAVL1)

ABSTRACT

Long noncoding RNAs (lncRNAs) modulate many aspects of biological and pathological processes. Recent studies have shown that host lncRNAs participate in the antiviral immune response, but functional lncRNAs in coxsackievirus B5 (CVB5) infection remain unknown. Here, we identified a novel cytoplasmic lncRNA, LINC1392, which was highly inducible in CVB5 infected RD cells in a time- and dose-dependent manner, and also can be induced by the viral RNA and IFN-β. Further investigation showed that LINC1392 promoted several important interferon-stimulated genes (ISGs) expression, including IFIT1, IFIT2, and IFITM3 by activating MDA5, thereby inhibiting the replication of CVB5 *in vitro*. Mechanistically, LINC1392 bound to ELAV like RNA binding protein 1 (ELAVL1) and blocked ELAVL1 interaction with MDA5. Functional study revealed that the 245–835 nt locus of LINC1392 exerted the antiviral effect and was also an important site for ELAVL1 binding. In mice, LINC1392 could inhibit CVB5 replication and alleviated the histopathological lesions of intestinal and brain tissues induced by viral infection. Our findings collectively reveal that the novel LINC1392 acts as a positive regulator in the IFN-I signaling pathway against CVB5 infection. Elucidating the underlying mechanisms on how lncRNA regulats the host innate immunity response towards CVB5 infection will lay the foundation for antiviral drug research.

1. Introduction

The innate immune system, especially the type I interferon (IFN-I) signaling pathway, is important as it is the first line of defense against viral infections (McNab et al., 2015). Viral nucleic acids are detected through pattern recognition receptors (PRRs), such as toll-like receptors (TLRs), retinoic acid-inducible gene I (RIG-I), and melanoma differentiation-associated gene 5 (MDA5). These receptors activate the adaptor signaling protein to form a complex with TANK-binding kinase (TBK) and IκB kinase ε (IKKε), which activates interferon regulatory factors (IRFs), induces its translocation into the nucleus, and triggers the rapid production of IFN-I (Kato et al., 2006; Wu and Chen, 2014). IFN-I stimulates the initiation of the Janus kinase/signal transducers and activators of transcription (JAK/STAT) signaling pathway, which induces the expression of many interferon-stimulated genes (ISGs), such as *OASL*, *MxA*, *ISG15*, *ISG20*, *IFIT1*, *IFIT2*, and *IFITM3*. The IFN-I signaling pathway is serving as an essential primary barrier against viral infection and promoting pathogen clearance (Darnell et al., 1994; Suarez et al., 2020).

Long noncoding RNAs (lncRNAs) are defined as transcripts longer than 200 nucleotides that lack a protein-coding function, and their expression levels are highly tissue- or cell-specific. Furthermore, the intracellular localization of the lncRNAs determines their individual functions (Wang and Chang, 2011). LncRNAs in the nucleus bind to target genes and activate or repress the expression of target genes by histone modification or by recruiting transcription factors (Fu et al., 2016). For example, NRAV, the ectopically expressed lncRNA in human cells or transgenic mice, promotes influenza A virus (IAV) replication through negatively regulates the ISG transcription, including IFITM3 and MxA via histone modification (Ouyang et al., 2014). In contrast, lncRNAs in the cytoplasm regulate intracellular signaling pathways by sponge or competitive binding to host proteins. IFN-I-inducible lncRNA-ISIR can compete with flightless-1(Fli-1), then facilitates IRF3-activation and strengthens interferon production in viral infection (Xu et al., 2021). Moreover, lncRNAs are a class of critical regulators in the signaling pathway, and widely participate in host-pathogen interactions (Ghafouri-Fard et al., 2022). However, the number of validated functional lncRNAs is still very limited, and in-depth studies on the roles of lncRNAs during viral infection are necessary.

Coxsackievirus B5 (CVB5) is a member of the genus *Enterovirus* in *Picornaviridae* family, with a single-strand positive-stranded RNA

* Corresponding author.
E-mail address: wchen@kust.edu.cn (W. Chen).

https://doi.org/10.1016/j.virs.2023.08.001
Received 25 August 2022; Accepted 21 July 2023
Available online 3 August 2023

genome (Yang et al., 2022). CVB5 causes hand-foot-and-mouth disease (HFMD) and poses a serious threat to the health of young children (Gao et al., 2018; Tsuno et al., 2018). CVB5 is known to invade the central nervous system leading to neurological symptoms, such as aseptic meningitis and acute flaccid paralysis, eventually resulting in death (Machado et al., 2022; Posnakoglou et al., 2021). Understanding the interactions between CVB5 and the host is vital for the development of drugs and vaccines.

The previous study analyzed the lncRNAs expression profiles of Rhabdomyosarcoma (RD) cells infected with CVB5 (Teng et al., 2022). The current study focused on a novel cytoplasmic lncRNA, LINC1392, which was a highly inducible in RD cells during CVB5 infection. Our results revealed that LINC1392 inhibited the replication of CVB5 through the activation of IFN-I signaling pathways. Further investigation showed that LINC1392 interacted with the embryonic lethal abnormal vision-like 1 (ELAVL1) protein and interrupted its negative regulation of MDA5 expression. *In vivo* investigation showed that LINC1392 acted as a positive regulator of innate antiviral immunity in mice, laying the foundation for developing clinical treatment for CVB5 infection.

2. Materials and methods

2.1. Cells and virus $TCID_{50}$ assay

RD cells, human epidermoid cancer Hep-2 cells, human neuroblastoma SH-SY5Y cells, human glioblastoma U251 cells, human embryonic kidney 293 (HEK-293T) cells, monkey kidney epithelial Vero cells, and mouse neuroblastoma N2A cells were cultured in Dulbecco's modified Eagle's medium (DMEM) (Hyclone, USA). HT29 cells were cultured in RPMI 1640 medium (Hyclone, USA). All the above culture mediums were supplemented with 10% (vol/vol) fetal bovine serum (FBS) (Gibco, USA). Cells were cultured at 37 °C under a humidified atmosphere of 5% CO_2 (Thermo Fisher Scientific, USA).

The CVB5 strain (GenBank accession no. MH201081.1) was isolated from an HFMD patient in Kunming, Yunnan Province, China, in 2014. Coxsackievirus A16 (CVA16) strain 74/YN/2016 (GenBank: KY440934.1), enterovirus A71 (EV71) strain RA330/YN/CHN/2009 (GenBank: MK028135.1), human alphaherpesvirus 1(HSV-1) isolate ZW6 (GenBank: KX424525.1), and influenza A virus (IAV) (A/Puerto Rico/8/1934(H1N1)) (GenBank: NC_002017.1) were stored in our laboratory. CVB5 was serially diluted from 10^{-1} to 10^{-15} with DMEM, and Vero cells were infected with the serial dilutions of CVB5. The cytopathic effect (CPE) was recorded for 5–7 days. The 50% tissue culture infectious dose ($TCID_{50}$) assay was calculated using the Reed-Muench method.

2.2. Antibodies and reagents

The following antibodies were purchased from Cell Signaling Technology (Danvers, MA, USA): MDA5 (#5321), Phospho-IRF-3 (#37829), Stat1 (#14994), Phospho-Stat1 (#7649), Anti-rabbit IgG (#7074) and Anti-mouse IgG (#7076). Additional antibodies purchased from ABclonal Technology Co., Ltd. (Wuhan, China) were: IRF3 (A19717) and ELAVL1 (A19622). CVB5-VP1 antibody (polyclonal, Rat) was prepared by our laboratory. Poly (I:C) high molecular weight (tlrl-pic, InvivoGen, Sorrento, San Diego, CA, USA) and recombinant human IFN-β (#300-02BC, PeproTech, Cranbury, NJ, USA) were prepared using sterile endotoxin-free physiological water.

2.3. Plasmids, siRNAs, and transfection

The LINC1392 sequence was cloned into pcDNA 3.1(+) plasmid for overexpression. LINC1392-specific siRNAs and negative control were synthesized by RiboBio Co., Ltd (Guangzhou, China). The target sequences of the siRNAs were as follows: si-LINC1392#01: CAACGGAGTATTCACAGTA; si-LINC1392#02: CACAGATACACTCCAGGAT; si-LINC1392#03: CTGGGTGAAACAGAAGTC. All transfections were carried out with the TransIntro™ EL Transfection Reagent (FT201, TRANSgene, Beijing, China).

2.4. Quantitative real-time PCR (qRT-PCR)

Total RNA was extracted from cells using RNAiso plus reagent (#9109, TaKaRa, Shiga, Japan). Reverse transcription and qRT-PCR analysis were performed using One-Step TB Green PrimeScript RT-PCR Kit (RR066A, Takara) with the following cycling conditions: 42 °C for 5 min, 95 °C for 5 s, followed by 40 cycles of 95 °C for 10 s and 60 °C for 34 s, extension and annealing at 95 °C for 15 s, 60 °C for 1 min. The GAPDH gene was used as an internal control, and the $2^{-\Delta\Delta Ct}$ method was used to calculate the relative RNA levels. All primers are shown in Supplementary Table S1.

2.5. Subcellular localization

The infected cells were separated into cytoplasmic and nuclear fractions using the PARIS Kit Protein and RNA Isolation System (AM1921, Invitrogen, Waltham, MA, USA). The cytoplasmic and nuclear fractions in cell fractionation buffer were centrifuged and the nuclear pellets were lysed with cell disruption buffer. RNA was extracted using 2× lysis/binding solution, and qRT-PCR was performed to detect the expression levels of LINC1392 in the cytoplasmic and nuclear fractions. GAPDH was used as the control gene for the cytoplasmic fractions, and U6 was used as the control gene for the nuclear fraction.

2.6. Western blotting

Total protein was extracted using radioimmunoprecipitation assay (RIPA) lysis buffer, and protein concentrations were calculated with the bicinchoninic acid (BCA) kit (PA115, TIANGEN, German). Protein were separated by sodium dodecyl sulfate-polyacrylamide gel electrophoresis (SDS-PAGE) and transferred onto polyvinylidene difluoride filter (PVDF) membranes. Protein bands were probed with specific antibodies and the antigen-antibody complexes were detected using an enhanced chemiluminescence (ECL) system (180-5001, Tanon, China).

2.7. RNA pull-down assay

Briefly, 1×10^7 RD cells were harvested and lysed using base lysis buffer plus 1% protease inhibitor (P1005, Beyotime, China) and 100 U/mL RNase inhibitor (R0102, Beyotime, China). Biotin-labeled LINC1392 was transcribed with the MEGAscript™ T7 Kit (AM1333, Thermo) and purified using the Monarch® RNA Cleanup Kit (T2050, New England Biolabs, Ipswich, MA, USA), then incubated with cell lysates at 37 °C for 1 h. The LINC1392 antisense strand was used as the control. According to the Pierce™ Magnetic RNA-Protein Pull-Down Kit (#20164, Thermo), the beads-Biotin RNA-protein complex was washed three times, followed by elution in loading buffer. The RNA complexes bound to these beads were boiled for Western blotting analysis.

2.8. RNA immunoprecipitation (RIP)

RD cells were collected and lysed with immunoprecipitation lysis buffer (25 mmol/L Tris-HCl, 150 mmol/L NaCl, 1 mmol/L EDTA, 5% glycerol, 1% NP-40) containing RNase inhibitor and protease inhibitor. RIP was performed using the Dynabeads™ Protein A Immunoprecipitation Kit (10006D, Thermo) following the manufacturer's instructions. The expression of LINC1392 was examined by qRT-PCR. Results were normalized to input RNA.

2.9. Co-immunoprecipitation (Co-IP)

RD cells were cultured and harvested at 24 h after transfection. Cells were lyzed with immunoprecipitation lysis buffer and incubated with

magnetic beads for 2 h at 4 °C on a rotator. The immune mixture was washed with buffer to remove the non-specific binding, and then added with loading buffer followed by boiling at 100 °C for Western blotting analysis.

2.10. In vivo experiments

BALB/c mice aged 0–2 weeks were purchased from Yunnan University (Kunming, China) and housed in a specific pathogen-free animal facility at the Experimental Animal Center of Kunming University of Science and Technology (Kunming, China). For LINC1392 overexpression in mice, a plasmid encoding 1392 was packaged into adeno-associated virus and named AAV2/9-CMV-LINC1392-zsgreen (AAV2/9-CMV-zsgreen as control) (NewHelix Biotech, Shanghai, China). BALB/c mice aged three days were infected with freshly purified virus (titer $\geq 2 \times 10^{11}$ IU/mL) via intraperitoneal injection for three times. After 14 days, the mice infected with CVB5 (20 LD50) by intraperitoneal injection. After 7 days, brain, intestinal and spleen were collected immediately for RT-qPCR and hematoxylin-eosin staining (HE) analysis to evaluate the CVB5 replication.

2.11. Statistical analysis

Data were expressed as mean ± standard deviation (SD) format. The student's *t*-test was carried out to analyze the data. $P < 0.05$ was considered statistically significant.

3. Results

3.1. Characterization of CVB5-induced LINC1392

LINC1392 is a long intergenic non-coding RNA transcribed from *XLOC_139471* located on chromosome 2q14.3 and is also referred to as TCONS_00270496 (Fig. 1A). Western blotting results showed that LINC1392 was not protein-coding (CVB5 non-structural protein 3C used as a control) (Fig. 1B). Upon CVB5 infection, the amount of cytoplasmic LINC1392 increased to 75% in RD cells (Fig. 1C). In addition, we observed that the expression level of LINC1392 was upregulated in RD cells in a virus infection dose- and time-dependent manner (Fig. 1D and E). Furthermore, LINC1392 was induced by the main HFMD pathogens, including EV71 and CVA16, but not by IAV or HSV-1 infection (Fig. 1F). Moreover, after CVB5 infection, LINC1392 was induced to be expressed in RD and HT-29 cells, but not in other human (SH-SY5Y, U251, and Hep-2) and mouse cell lines (N2A) (Fig. 1G).

3.2. LINC1392 was induced by viral RNA and interferon-regulated

To investigate the key factor for LINC1392 activation, RD cells were stimulated by the cellular RNA derived from uninfected cells, viral RNA, and CVB5 nonstructural proteins (2B/2C/3AB/3C/3D). The results showed that the expression of LINC1392 was positively regulated by viral RNA, but not by the cellular RNA or CVB5 nonstructural proteins (Fig. 2A and B). To further verify that viral RNA was a critical factor responsible for the induction of LINC1392, we tested LINC1392 expression in response to poly (I:C). As shown in Fig. 2C, the expression of LINC1392 was dramatically induced by poly (I:C) in a low dose-dependent manner. Furthermore, the data showed that the expression level of LINC1392 was significantly higher in IFNβ-treated cells (Fig. 2D). These data suggested that LINC1392 was an interferon-regulated LncRNA and the increment level was associated with viral RNA accumulation during the viral replication.

3.3. LINC1392 suppressed CVB5 replication in vitro

LINC1392 was upregulated during viral infection, we sought to determine the role of LINC1392 in CVB5 replication. LINC1392 overexpressing plasmid was generated based on the pcDNA3.1 expression vector (Fig. 3A). CVB5 VP1 expression and $TCID_{50}$ assay results demonstrated that CVB5 replication was impaired in RD cells that overexpressed LINC1392 (Fig. 3B and C). We also generated specific siRNAs targeting LINC1392. As shown in Fig. 3D, si-LINC1392#03 exhibited a high efficiency, and the knockdown of LINC1392 promoted CVB5 replication (Fig. 3E and F). These data suggested that LINC1392 suppressed the replication of CVB5 *in vitro*.

3.4. LINC1392 activated the expression of ISGs and the IFN-I pathway

IFN-I is the first line of antiviral immune response following virus infection. Thus, we investigated whether LINC1392 affected the expression of IFN-β and ISGs. RD cells were transfected with si-LINC1392#03 or pcDNA3.1-LINC1392 plasmid and cultured for 24 h. Then the cells were infected with CVB5 (MOI = 1), and the mRNA expression level of IFN-β and vital ISGs was determined at 24 hours post-infection (hpi). The results showed that knockdown of LINC1392 down-regulated the levels of IFN-β and ISGs (Fig. 4A), while overexpression of LINC1392 promoted the expression of the levels of IFN-β and ISGs (Fig. 4B), indicating that LINC1392 is a positive regulator of IFN-I downstream factors during CVB5 infection *in vitro*. To explore the effects of LINC1392 in regulating the IFN-I signaling pathway, we examined the expression of the key proteins in this pathway, including PRRs (MDA5) and key adaptors (IRF3 and STAT1). Knockdown of LINC1392 strongly suppressed the expression of MDA5, p-IRF3, and p-STAT1 levels upon CVB5 infection (Fig. 4C). In contrast, overexpression of LINC1392 promoted the expression levels of MDA5, p-IRF3 and p-STAT1 (Fig. 4D). Also, in the MDA5 knocked down cells, the expression of LINC1392 was impaired (Supplementary Fig. S1). Together, the results suggested that LINC1392 enhanced host antiviral immunity by regulating the MDA5, which activated the p-IRF3 and p-STAT1 that then triggered IFN-JAK-STAT signaling and the expression of ISGs to inhibit viral replication.

3.5. LINC1392 directly bind to ELAVL1 protein and blocked ELAVL1-MDA5 interaction

Studies have shown that cytoplasm lncRNAs bind to proteins to exert their function. We firstly confirmed LINC1392 was not associated with MDA5 using the RNA pull-down assay (Supplementary Fig. S2). Then we predicted the proteins interacting with LINC1392 using catRAPID (http://service.tartaglialab.com/page/catrapid_group) and obtained eight proteins as candidates (Supplementary Table S2). Based on the functional analysis and literature, we selected the ELAVL1 protein to serve as a candidate protein. RNA pull-down analysis was performed to verify the interaction between LINC1392 and ELAVL1 protein, and the results confirmed that LINC1392 was bound to ELAVL1 (Fig. 5A). We also performed the RIP assay using anti-ELAVL1 antibody or the isotype control in RD lysates to validate the pull-down analysis. Enrichment of LINC1392 was observed in the immunoprecipitated sample using the anti-ELAVL1 antibody compared to the isotype control antibody (Fig. 5B). We further observed that the ELAVL1 was associated with MDA5 after CVB5 infection (Fig. 5C). Meanwhile, ELAVL1 promoted viral replication and as a MDA5 negative regulatory (Fig. 5D). Then the autophagy inhibitor (3MA and CQ), the caspase inhibitor (Z-VAD-FMK), and the proteasome inhibitor (MG132) were used to evaluate the mechanism of ELAVL1 down-regulated the MDA5. The result showed that the ELAVL1 inhibit the expression of MDA5 through the autophagosome-lysosome pathway (Fig. 5E). Additionally, RD cells were transfected with the si-LINC1392 and the Co-IP showed that LINC1392 could inhibit the binding of ELAVL1 and MDA5 after CVB5 infection (Fig. 5F). Furthermore, the RD cells were transfected with both the si-LINC1392 and siRNA ELAVL1, the MDA5 and VP1 expression recovered (Fig. 5G). Together, these data suggested that LINC1392 functioned through ELAVL1.

3.6. The 245–835 nt site of LINC1392 was the functional main site

It is well known that secondary structures are highly associated with the diverse functions of lncRNA. We further dissected the functional structures of LINC1392. Four major sub-structures with base-paired and hairpin structures were successfully constructed according to the secondary structure of LINC1392 predicted by the RNAfold web server (Fig. 6A). We cloned the segments of LINC1392 corresponding to the four sub-structures (LINC1392-1, LINC1392-2, LINC1392-3, LINC1392-4) into pcDNA3.1 (Fig. 6B). Truncated LINC1392 segments were transfected

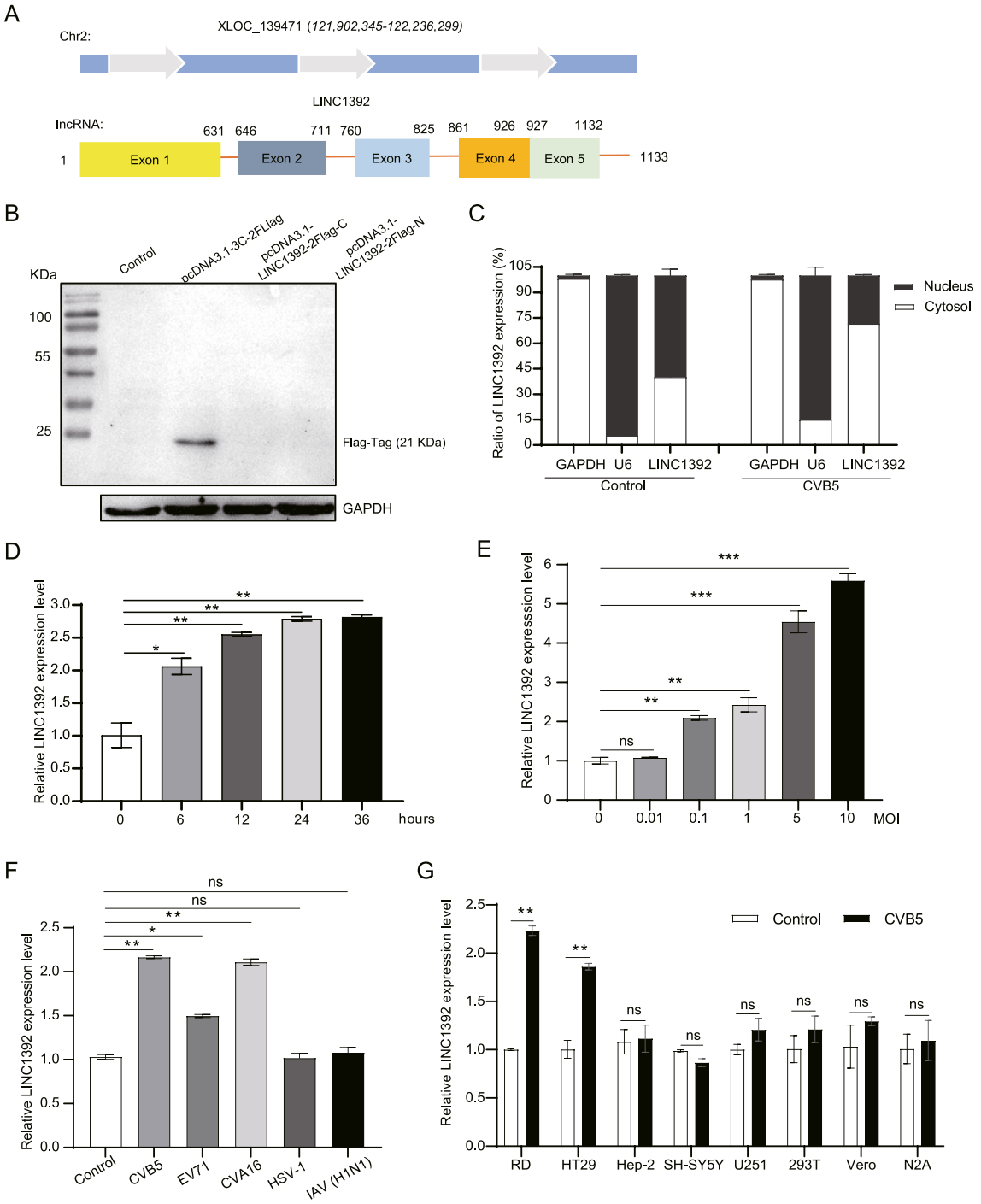

Fig. 1. The features of LINC1392. **A** Schematic representation of human LINC1392 transcribed from the *XLOC_139471* gene. **B** Western blotting was used to assess LINC1392 protein-coding ability. pcDNA3.1-2Flag-3C, pcDNA3.1-LINC1392-2Flag-C, pcDNA3.1-LINC1392-2Flag-N plasmid (2.0 μg) or control (pcDNA3.1) were transfected into HEK293T cells. After 24 h, cells were collected and analyzed by Western blotting with Flag antibody. **C** CVB5 (MOI = 1) infected RD cells for 24 h (mock infected as control), cells were collected and separated the cytoplasmic and nuclear fractions. The expression levels of LINC1392 in different subcellular fractions were determined by qRT-PCR. GAPDH and U6 mRNA were respectively used as cytoplasmic and nuclear control. **D** Levels of LINC1392 were determined by qRT-PCR after RD cells were infected with CVB5 (MOI = 1) for the indicated time intervals. **E** Levels of LINC1392 were determined by qRT-PCR after RD cells were infected with indicated MOIs of CVB5 for 24 h. **F** Levels of LINC1392 were determined by qRT-PCR after RD cells were infected with CVB5, CVA16, EV71, HSV-1 and IAV (MOI = 1) for 24 h. **G** Levels of LINC1392 were determined by qRT-PCR in indicated cells lines infected with CVB5 (MOI = 1) for 24 h. Biologically independent experiments (n = 3) were conducted and all data are shown as mean ± SD. The student's *t*-test was performed, $^{*}P < 0.05$, $^{**}P < 0.01$ and $^{***}P < 0.001$; ns, not significant.

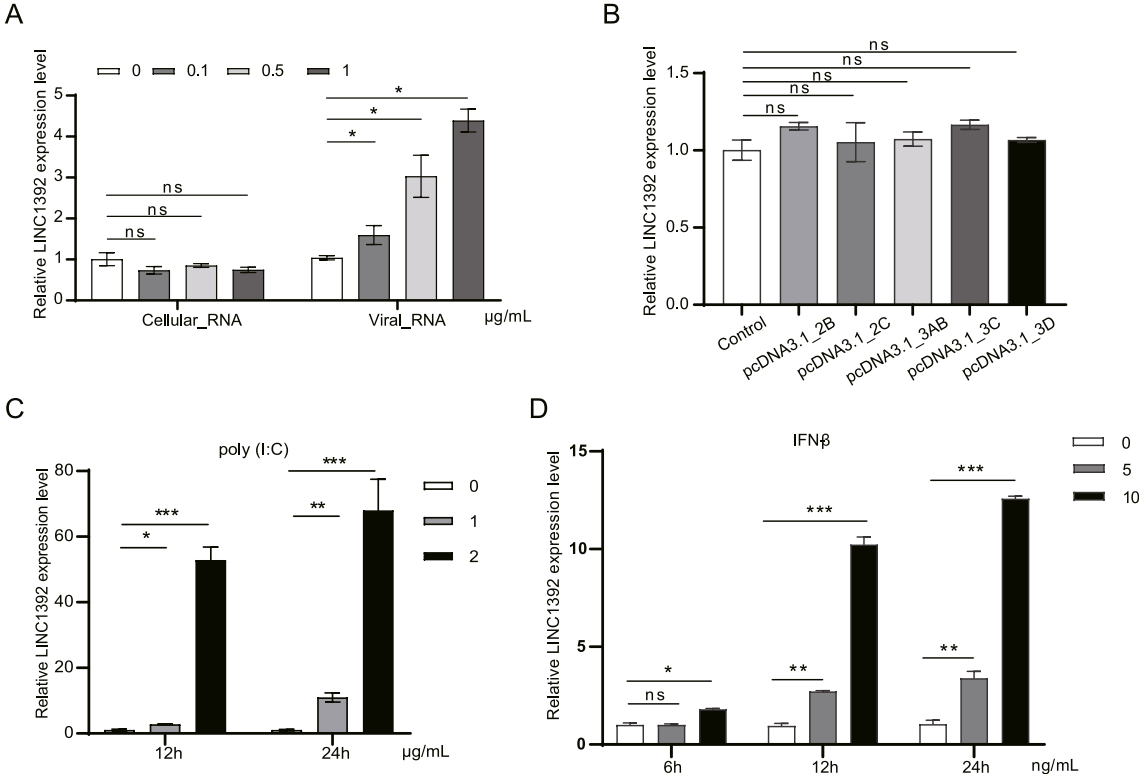

Fig. 2. LINC1392 is an inducible host lncRNA. **A** RD cells were transfected with different amounts of cellular RNA or viral RNA. Levels of LINC1392 were determined by qRT-PCR at 24 h post-transfection. **B** RD cells which were transfected with different viral nonstructural protein plasmids (2.0 μg). Levels of LINC1392 were determined by qRT-PCR at 24 h post-transfection. **C** Expression level of LINC1392 in RD cells transfected with different amounts of poly (I:C) was determined by qRT-PCR at 12 and 24 h post-transfection. **D** Expression level of LINC1392 in RD cells treated with different amounts of IFN-β was determined by qRT-PCR at 6, 12 and 24 h post-transfection. Biologically independent experiments (n = 3) were conducted and all data are shown as mean ± SD. The student's *t*-test was performed, $^{*}P < 0.05$, $^{**}P < 0.01$ and $^{***}P < 0.001$; ns, not significant..

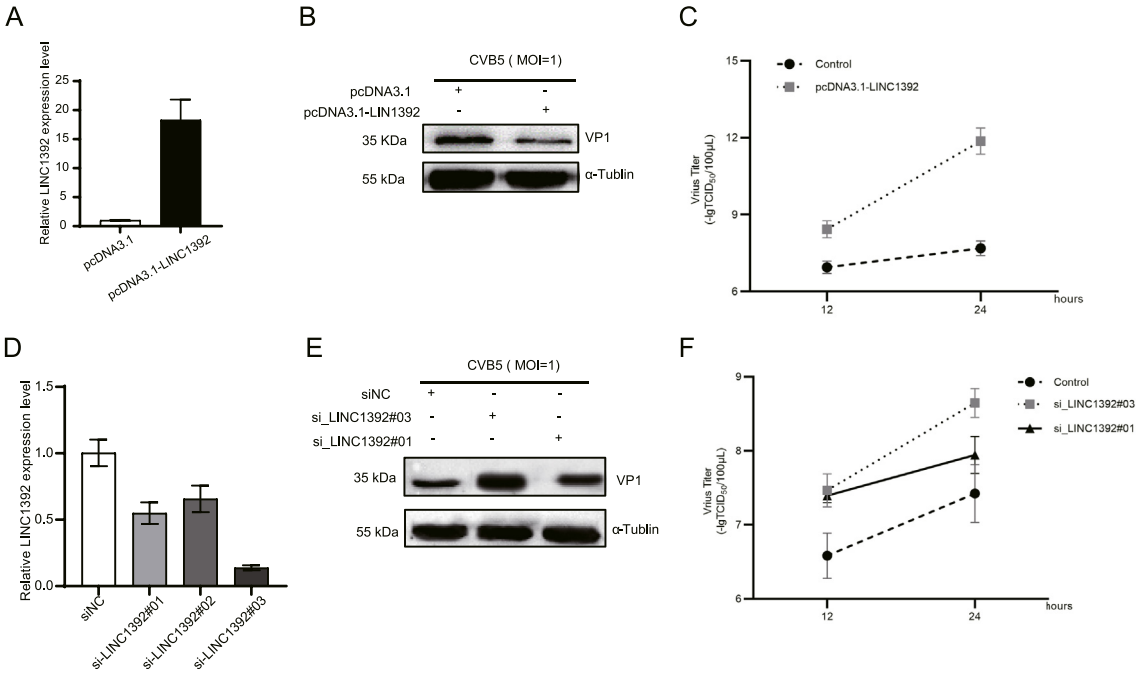

Fig. 3. LINC1392 inhibits CVB5 replication. **A–C** pcDNA3.1-LINC1392 plasmid (2.0 μg) or empty vector (pcDNA3.1) were transfected into RD cells, and the cells were infected with CVB5 (MOI = 1) at 24 h after transfection. Cells were harvested at 24 hours post-infection (hpi), the expression levels of LINC1392 were determined by qRT-PCR (**A**), and the expression level of CVB5 VP1 protein were determined by Western blotting (**B**). The supernatant was collected at 12 and 24 hpi, and the CVB5 titers were determined by $TCID_{50}$ assay (**C**). **D** si_LINC1392#01, si_LINC1392#02, si_LINC1392#03 (50 nmol/L) or empty vector (siNC) was transfected into RD cells, then the cells were infected with CVB5 (MOI = 1) at 24 h after transfection. The expression levels of LINC1392 were determined by qRT-PCR at 24 hpi. **E–F** si_LINC1392#03, si_LINC1392#01 (50 nmol/L) or empty vector (siNC) was transfected into RD cells, then the cells were infected with CVB5 (MOI = 1) at 24 h after transfection. The expression level of CVB5 VP1 protein were determined by Western blotting at 24 hpi (**E**). The supernatant was collected at 12 and 24 hpi, CVB5 titers were determined by $TCID_{50}$ assay (**F**). Data are represented as mean ± SD.

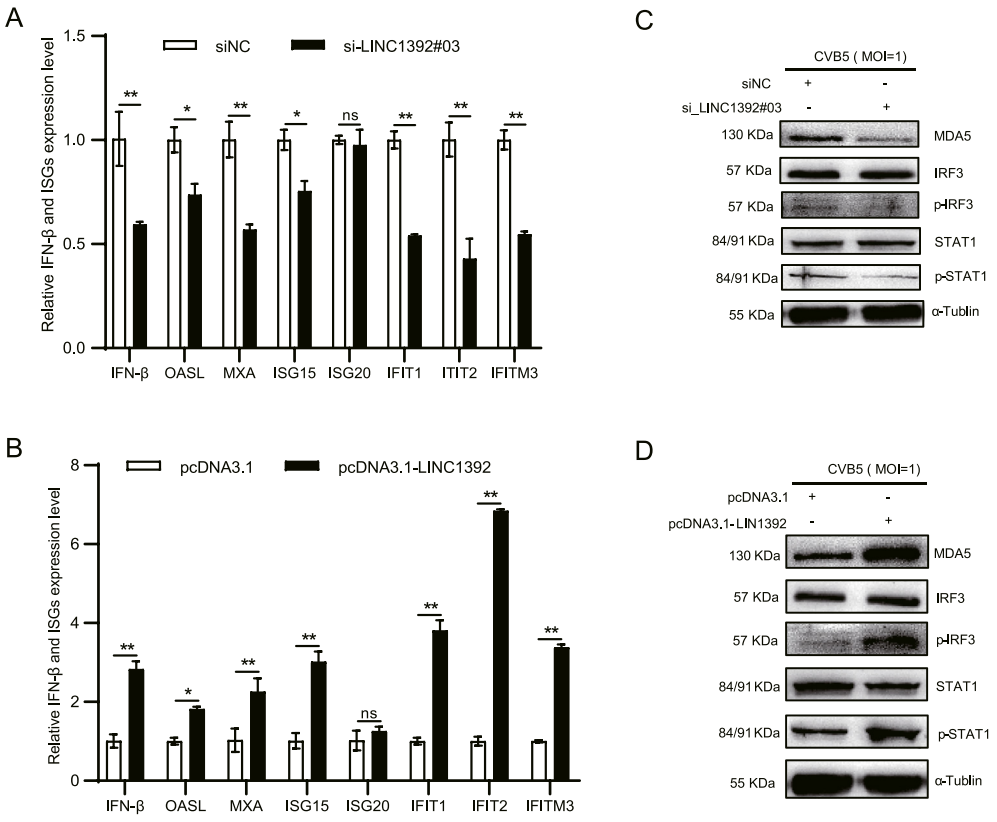

Fig. 4. LINC1392 activated ISGs expression and IFN-I pathway via regulating MDA5. **A** si_LINC1392#03 (50 nmol/L) or empty vector (siNC) were transfected into RD cells, then the cells were infected with CVB5 (MOI = 1) at 24 h after transfection. Cells were harvested at 24 h.p.i., qRT-PCR was performed to determine the mRNA expression of vital ISGs, and IFNβ. **B** pcDNA3.1-LINC1392 plasmid (2.0 μg) or empty vector (pcDNA3.1) were transfected into RD cells, and the cells were infected with CVB5 (MOI = 1) at 24 h after transfection. Cells were harvested at 24 h.p.i., qRT-PCR was performed to determine the mRNA expression of vital ISGs, and IFNβ. **C** si_LINC1392#03 (50 nmol/L) or empty vector (siNC) were transfected into RD cells, then the cells were infected with CVB5 (MOI = 1) at 24 h after transfection. Cells were harvested at 24 h.p.i., the expression level of MDA5, IRF3 (p-IRF3) and STAT1 (p-STAT1) were determined by Western blotting. **D** pcDNA3.1-LINC1392 plasmid (2.0 μg) or empty vector (pcDNA3.1) were transfected into RD cells, then the cells were infected with CVB5 (MOI = 1) at 24 h after transfection. Cells were harvested at 24 h.p.i., the expression level of MDA5, IRF3 (p-IRF3) and STAT1 (p-STAT1) were determined by Western blotting. Biologically independent experiments (n = 3) were conducted and all data are shown as mean ± SD. The student's *t*-test was performed, $^{*}P < 0.05$ and $^{**}P < 0.01$; ns, not significant.

in RD cells, and the cells were infected with CVB5 (MOI = 1) at 24 h post-transfection. The stem-loops in LINC1392-2 (245–835 nt) exerted inhibitory effect in the CVB5 replication (Fig. 6C). The RIP assay showed that LINC1392-2 (245–835 nt) might form a spatial structure which is essential for the interaction with ELAVL1 (Fig. 6D).

3.7. LINC1392 inhibited CVB5 replication and alleviated the pathological lesions in mice

To verify the role of LINC1392 *in vivo*, we overexpressed LINC1392 in BALB/c mice (Fig. 7A). After AAV2/9-CMV-LINC1392-zsgreen injection 14 days, LINC1392 was indeed highly expressed in brain, intestine, and spleen (Supplementary Fig. S3). Then, the mice were infected with CVB5 (20 LD50) by intraperitoneal injection and tissue samples were collected at day 7 post-infection. In LINC1392 overexpression group, the CVB5 VP1 expression level was reduced in most of the organs (Fig. 7B), and the IFN-β and ISGs mRNA was increased in brain, intestine and spleen compared to controls (Fig. 7C). Meanwhile, HE staining showed significantly reduced lesions in the intestine and brain tissues of the mice (Fig. 7D). Together, these data suggest that overexpression of LINC1392 in mice could inhibit CVB5 replication and alleviate the pathological lesions of intestinal and brain tissues after viral infection.

4. Discussion

Studies have demonstrated that lncRNAs play important roles in the innate immunity response to virus infection (Zhang and Cao, 2016). However, the involvement of lncRNAs in the innate immune response to CVB5 infection remains largely unknown, and the mechanisms are poorly understood. In the previous study, we identified the lncRNA expression profiles in RD cells infected with CVB5 and found a novel upregulated lncRNA, LINC1392 (Teng et al., 2022). In this study, we further elucidated the role of LINC1392 during CVB5 infection. LINC1392 inhibited the CVB5 infection by enhancing the expression of IFN-β and several ISGs to activate the IFN-I signaling pathway, which strengthened MDA5 expression through interaction with ELAVL1. Notably, multiple stem ring arms of LINC1392 may form a stable spatial structure and are required for its antiviral activity. One main functional domain of LINC1392 which we identified is the stretch of nucleotides from 245 to 835 nt. *In vivo*, LINC1392 also inhibited the CVB5 replication and then alleviated pathological changes. Our results have demonstrated for the first time the lncRNA antiviral immune mechanism in the fight against CVB5 infection.

LINC1392 is an intergenic lncRNA and locates on chromosome 2q14.3. It has no protein-coding ability consistent with the non-coding function of most lncRNAs (Fig. 1B) (Zhao et al., 2020). LncRNA

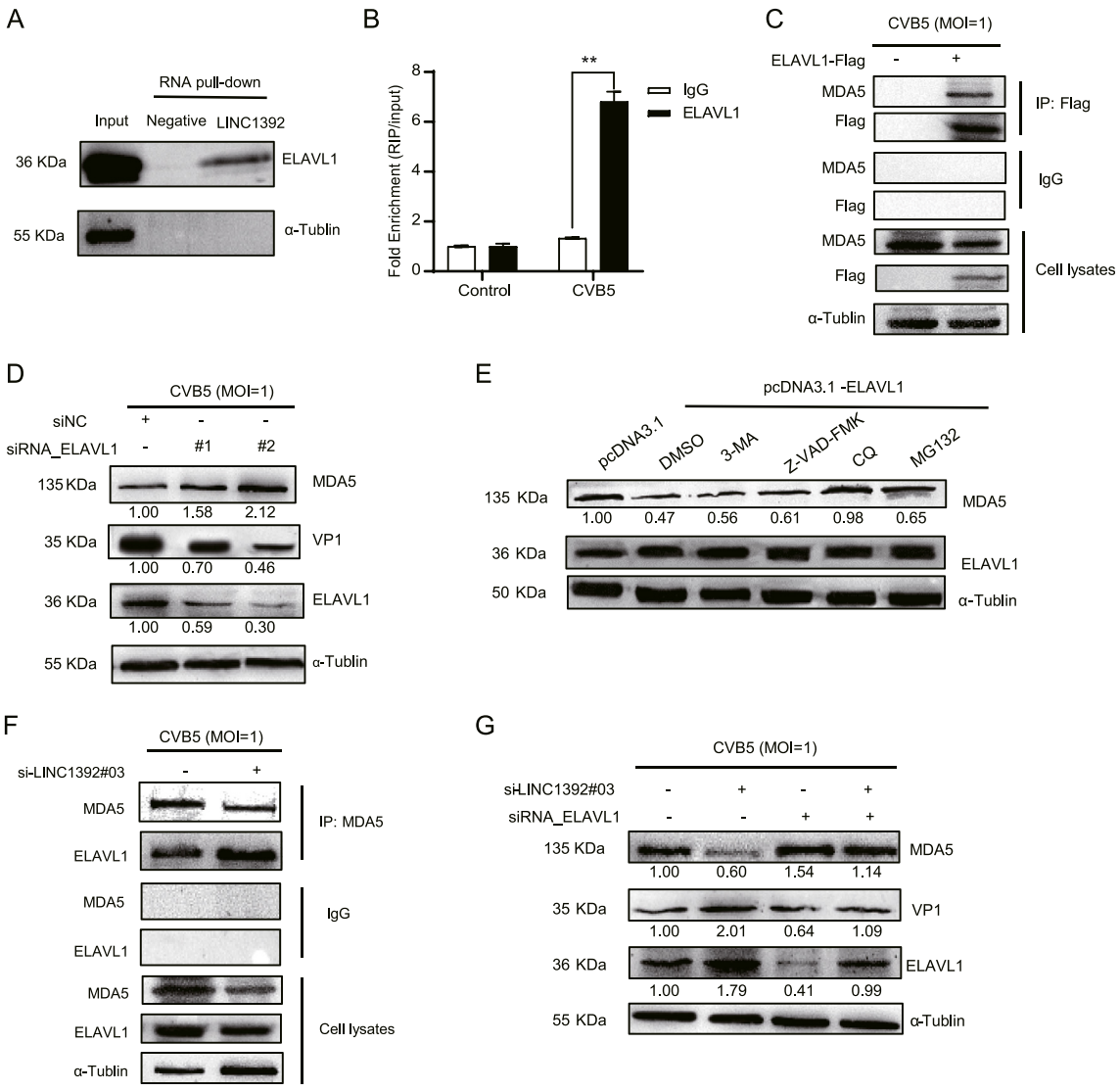

Fig. 5. LINC1392 directly binds to ELAVL1 protein. **A** RNA pull-down analysis of LINC1392 binding to ELAVL1. CVB5 (MOI = 1) infected RD cells and cells were harvested 24 hours post-inhibition (hpi). Cell lysis, the biotinylated LINC1392 positive strand (50 pmol) and magnetic beads were incubated at 25 °C to obtain the protein-RNA complexes. The biotin-labeled LINC1392 negetivative chain was used as control. Samples were loaded on 10% SDS-PAGE gel and subjected to ELAVL1 Western blotting. **B** The association of LINC1392 and ELAVL1 was confirmed by RNA immunoprecipitation (RIP)-qPCR. CVB5 (MOI = 1) infected RD cells (mock infected as control) and cells were harvested at 24 hpi. Cell lysates, the ELAVL1 antibody (IgG as control) and magnetic beads were incubated at 4 °C overnight to obtain the protein-RNA complexes. Extracted the total RNA, and the expression levels of LINC1392 were determined by qRT-PCR (%input). **C** pcDNA3.1-ELAVL1-2Flag (2.0 μg) or empty vector (pcDNA3.1) were transfected into RD cells, and the cells were infected with CVB5 (MOI = 1) 24 h after transfection. Cells were harvested at 24 hpi, and the Co-IP analysis was conducted to determine the interaction between ELAVL1 and MDA5. **D** siRNA_ELAVL1#1, siRNA_ELAVL1#2 (50 nmol/L) or empty vector (SiNC) were transfected into RD cells, and the cells were infected with CVB5 (MOI = 1) 24 h after transfection. Cells were harvested at 24 hpi, the expression level of CVB5 VP1, MDA5 and ELAVL1 were determined by Western blotting. **E** RD cells were transfected with 2.0 μg of pcDNA3.1-ELAVL1-2Flag for 24 h and infected with CVB5 (MOI = 1) for another 24 h. Cells maintained for 48 h in the presence of the autophagy inhibitor (3MA and CQ), the caspase inhibitor (Z-VAD-FMK), or the proteasome inhibitor (MG132). The expression of MDA5 was determined by Western blotting. **F** si_LINC1392#03 (50 nmol/L) or empty vector (siNC) were transfected into RD cells, then the cells were infected with CVB5 (MOI = 1) 24 h after transfection. Cells were harvested at 24 hpi, and the Co-IP analysis was conducted to determine the interaction between ELAVL1 and MDA5. **G** si_LINC1392#03 (50 nmol/L) or/and siRNA-ELAVL1#2 (50 nmol/L) were transfected into RD cells, and the cells were infected with CVB5 (MOI = 1) 24 h after transfection. Cells were harvested at 24 hpi, the expression level of MDA5, CVB5 VP1 and ELAVL1 were determined by Western blotting. The band intensity of proteins was quantified and the ratios of the target protein (MDA5, VP1 or ELAVL1) to α-Tublin were calculated.

distribution is cell- or tissue-specific (Yao et al., 2022), and LINC1392 was upregulated only in RD and HT-29 cells, but not in human or mouse neuronal cells (Fig. 1G). In addition, LINC1392 exhibited a time-dose dependence on CVB5 infection, suggesting its possible involvement in viral pathogenesis (Fig. 1D and E). Also, we observed that the expression of LINC1392 was significantly enhanced upon infection of EV71, CVA16, and CVB5 (Fig. 1F). The results indicated that LINC1392-related cellular response might be a specific defense against HFMD virus infection. Furthermore, we demonstrated that LINC1392 was induced by viral RNA but not viral nonstructural proteins (Fig. 2A and B). Poly (I:C) as the double-stranded RNA mimics recognized TLR3 or MDA5 further validating the previous results (Fig. 2C) (Bardel et al., 2016). The expression of LINC1392 was affected by IFN-β stimulation which indicated it was interferon-regulated (Fig. 2D). Our findings have offered a novel perspective different from the study of specific protein molecules involved in CVB5 infection.

Next, we demonstrated that LINC1392 was a functional molecule, which inhibited the CVB5 replication (Fig. 3). The innate immune is the

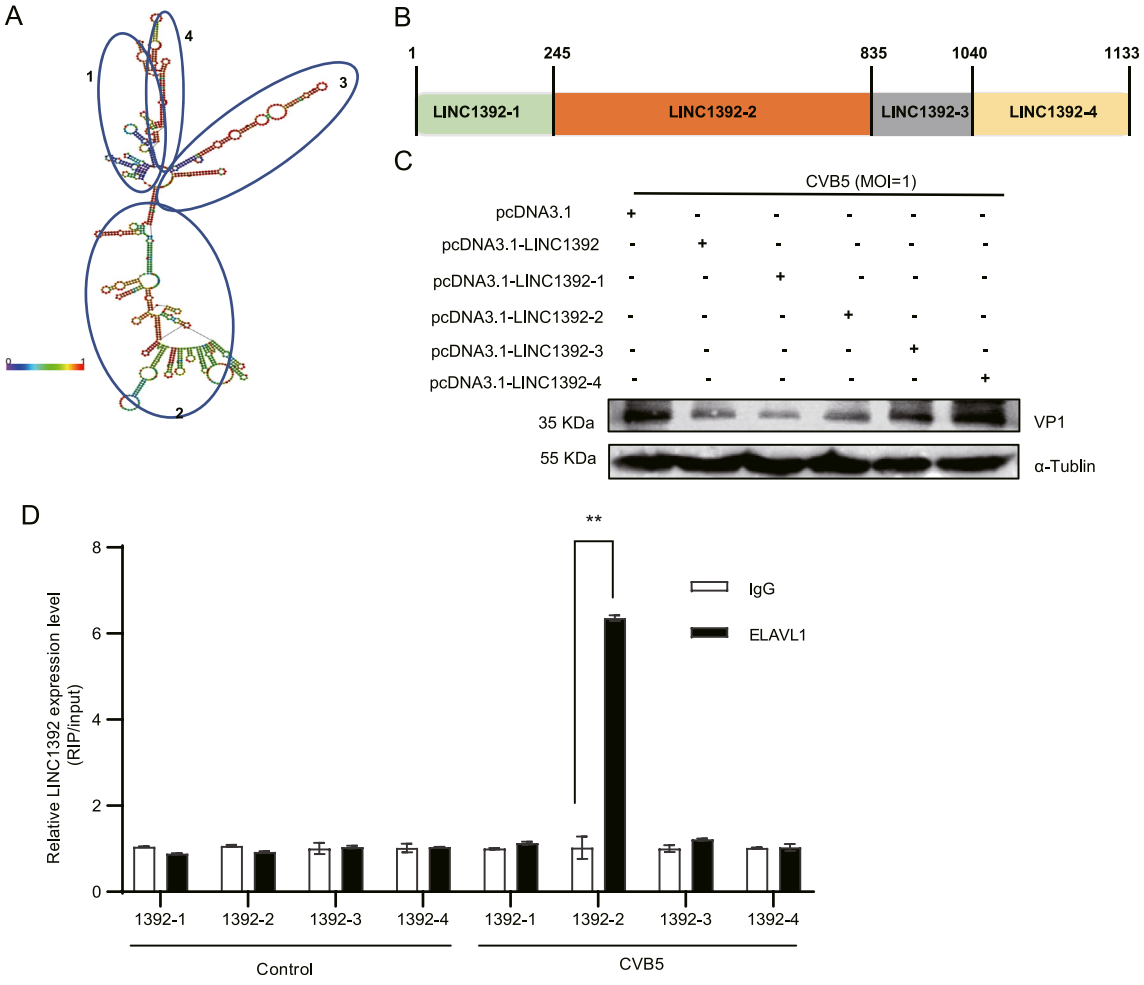

Fig. 6. The 245-835 nt site of LINC1392 was the functional main site. **A** Secondary structure of LINC1392 analyzed using RNAfold (Base pairing probabilities are color-coded on a scale from 0 (blue) to 1 (red)). **B** A schematic diagram of the truncated functional domain of LINC1392 is shown. **C** pcDNA3.1-LINC1392 (2.0 μg), its truncated functional domain (pcDNA3.1-LINC1392-1, pcDNA3.1-LINC1392-2, pcDNA3.1-LINC1392-3, pcDNA3.1-LINC1392-4) plasmid or empty vector (pcDNA3.1) were transfected into RD cells, then the cells were infected with CVB5 (MOI = 1) 24 h after transfection. Cells were harvested at 24 hpi, the expression level of CVB5 VP1 protein were determined by Western blotting. **D** RD cells were infected with CVB5 at the MOI of 1, and cells were harvested at 24 hpi (mock infected as control). Cell lysates, the ELAVL1 antibody (IgG as control), and magnetic beads were incubated at 4 °C overnight to obtain the protein-RNA complexes. The expression levels of LINC1392 truncated functional domain in extracted total RNA were determined by qRT-PCR (%input). Data are represented as mean ± SD. The student's *t*-test was performed, $^{**}P < 0.01$.

first line against the virus infection, and the IFN-I signaling pathway is known to be activated upon RNA virus infections and is involved in the induction and regulation of the innate immune response (Chen et al., 2017). LncRNA, as the "switch" that regulates the IFN-I innate immune pathway, can play a role in the expression and activation of PRRs, IFN gene transcription, ISGs expression, and other immune responses. For example, lnc-lsm3b regulated viral replication by competing with viral RNA for binding to RIG-I, which restricted protein conformational changes and downstream signal transduction (Jiang et al., 2018); lncRNA GM indirectly interacted with kinase TBK1 to regulate viral replication (Wang et al., 2020); lncRNA-CMPK2 inhibited viral replication by regulating ISGs expression (Gao et al., 2020). In our research, the expression of several key ISGs, such as IFIT1, IFIT2, and IFITM3, was reduced after knockdown of LINC1392 (Fig. 4A). It suggested that LINC1392 regulated CVB5 replication by affecting ISGs expression. Our results further indicated that LINC1392 could positively regulate the IFN-I signaling pathway by regulating MDA5 (Fig. 4CD). Together, these findings establish that LINC1392 functions as an important regulatory molecule that modulates the host's innate immune response against CVB5 infection via positively regulating the expression of MDA5 and then activating the expression of key ISGs.

Molecular mechanisms of lncRNA function are associated with their subcellular localization (Chai et al., 2018; Sui et al., 2020; Wang et al., 2018). Our data showed that LINC1392 was predominantly localized to the cytoplasm, suggesting that LINC1392 may exert its biological function by interacting with RNA-binding proteins. The present study uncovered that LINC1392 directly binds to ELAVL1 and also was a key negative regulator in the expression regulation of MDA5 via LINC1392 (Fig. 5 and Supplementary Fig. S2). ELAVL1, known as human antigen R (HuR), is an RNA binding protein and ubiquitously expressed in all tissues. As an RNA regulator, ELAVL1 competes for gene sites that typically contains AU-rich elements (AREs) in the 3′ untranslated region (UTR), thereby mediates the expression of various proteins by post-transcriptional mechanisms (Rothamel et al., 2021; Liu et al., 2020). In addition, the importance of ELAVL1-mediated roles in cancer development and progression has been thoroughly studied. In normal tissues, ELAVL1 exists in the form of nuclear expression, while in some tumor tissues, the cytoplasmic ELAVL1 expression level is significantly enhanced, and the cytoplasmic ElAVL1 expression level is positively correlated with tumor grade (Palomo-Irigoyen et al., 2020; Young et al., 2009; Yu et al., 2020). What's more, ELAVL1 has been attracted a great deal of

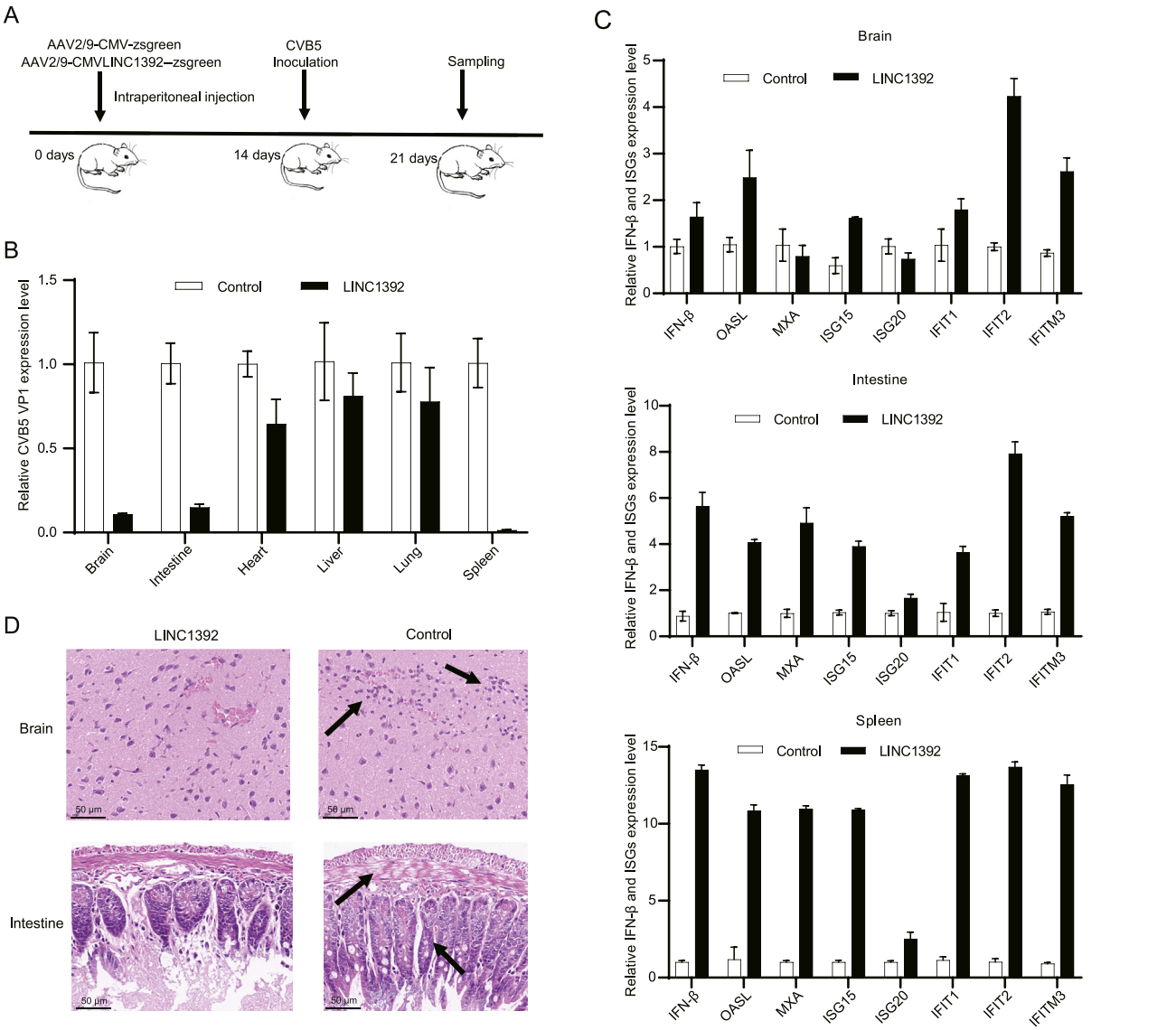

Fig. 7. LINC1392 inhibited the CVB5 replication and alleviated the pathological lesions *in vivo*. **A** Schematic diagram for *in vivo* experiments. Three-day-old BALB/c mice were infected with AAV2/9-CMV-LINC1392-zsgreen (2×10^{11} IU/mL) or AAV2/9-CMV-zsgreen (2×10^{11} IU/mL) via intraperitoneal injection for three times. After 14 days, the mice infected with CVB5 (20 LD50) by intraperitoneal injection. Samples were collected at 7 days post infection. **B** qRT-PCR was performed to determine the mRNA expression of CVB5 VP1 in different tissues. **C** qRT-PCR was performed to determine the mRNA expression of IFN-β and ISGs after the expression of LINC1392 in brain, intestine and spleen. **D** Hematoxylin-eosin staining was used to evaluate the pathological condition after the expression of LINC1392 in brain and intestine. Six BALB/c for the experimental group, and independently replicated three times.

attention in viral infections currently. ELAVL1 protein promoted viral replication in adenovirus infections (Jehung et al., 2018), but exerted antiviral effects in Zika virus infections (Bonenfant et al., 2019). Our results showed that ELAVL1 promoted the CVB5 replication as a negative regulatory in MDA5-mediated signaling pathway, but this effect could be interrupted by lncRNA-LINC1392. That might provide some clues for the lncRNAs function studies on innate antiviral immunity. However, there is still a substantial gap between the current understandings of the potential roles of ELAVL1 in the progression of viral replication.

5. Conclusions

Taken together, we identified a novel host lncRNA-LINC1392 which suppressed CVB5 replication by targeting ELAVL1 to regulate the activation of MDA5-mediated host antiviral innate immunity. This unique regulation mode has enabled us to understand the precise control of host immune homeostasis. Our study shed new insights into the complex mechanisms of how host antiviral immunity is regulated by lncRNAs.

Data availability

All data generated or analyzed in the study are included in this published paper.

Ethics statement

All animal experiments were approved by the Institutional Animal Care and Use Committee at the Kunming University of Science and Technology. All institutional and national guidelines for the care and use of laboratory animals were followed.

Author contributions

Jing Li: methodology, formal analysis, writing-original draft. Jinwei Li: methodology, formal analysis, software. Peiying Teng: methodology, formal analysis, software. Fan Yang: methodology. Jihong Zhang: writing reviewing. Bo Sun: writing reviewing. Wei Chen: conceptualization, supervision, writing-original draft. All authors approved the final version of the manuscript.

Conflict of interest

The authors declare that they have no conflict of interest.

Acknowledgements

This work was supported by the National Natural Science Foundation of China (No. 81860357), and the Young Talents Support Program of Yunnan Province, China (Ten Thousand People Plan, YNWR-QNBJ-2019-178).

Appendix A. Supplementary data

Supplementary data to this article can be found online at https://doi.org/10.1016/j.virs.2023.08.001.

References

Bardel, E., Doucet-Ladeveze, R., Mathieu, C., Harandi, A.M., Dubois, B., Kaiserlian, D., 2016. Intradermal immunisation using the TLR3-ligand Poly (I:C) as adjuvant induces mucosal antibody responses and protects against genital HSV-2 infection. NPJ Vaccines 1, 16010.

Bonenfant, G., Williams, N., Netzband, R., Schwarz, M.C., Evans, M.J., Pager, C.T., 2019. Zika virus subverts stress granules to promote and restrict viral gene expression. J. Virol. 93, e00520-19.

Chai, W., Li, J., Shangguan, Q., Liu, Q., Li, X., Qi, D., Tong, X., Liu, W., Ye, X., 2018. LncISG20 inhibits influenza A virus replication by enhancing ISG20 expression. J. Virol. 92, e00539-18.

Chen, Y.G., Satpathy, A.T., Chang, H.Y., 2017. Gene regulation in the immune system by long noncoding RNAs. Nat. Immunol. 18, 962–972.

Darnell Jr., J.E., Kerr, I.M., Stark, G.R., 1994. Jak-STAT pathways and transcriptional activation in response to IFNs and other extracellular signaling proteins. Science 264, 1415–1421.

Fu, M., Zou, C., Pan, L., Liang, W., Qian, H., Xu, W., Jiang, P., Zhang, X., 2016. Long noncoding RNAs in digestive system cancers: functional roles, molecular mechanisms, and clinical implications (Review). Oncol. Rep. 36, 1207–1218.

Gao, F., Bian, L., Hao, X., Hu, Y., Yao, X., Sun, S., Chen, P., Yang, C., Du, R., Li, J., Zhu, F., Mao, Q., Liang, Z., 2018. Seroepidemiology of coxsackievirus B5 in infants and children in Jiangsu province, China. Hum. Vaccin. Immunother. 14, 74–80.

Gao, Q., Zhou, R., Meng, Y., Duan, R., Wu, L., Li, R., Deng, F., Lin, C., Zhao, L., 2020. Long noncoding RNA CMPK2 promotes colorectal cancer progression by activating the FUBP3-c-Myc axis. Oncogene 39, 3926–3938.

Ghafouri-Fard, S., Poornajaf, Y., Dashti, F., Hussen, B.M., Taheri, M., Jamali, E., 2022. Interaction between non-coding RNAs and interferons: with an especial focus on type I interferons. Front. Immunol. 13, 877243.

Jehung, J.P., Kitamura, T., Yanagawa-Matsuda, A., Kuroshima, T., Towfik, A., Yasuda, M., Sano, H., Kitagawa, Y., Minowa, K., Shindoh, M., Higashino, F., 2018. Adenovirus infection induces HuR relocalization to facilitate virus replication. Biochem. Biophys. Res. Commun. 495, 1795–1800.

Jiang, M., Zhang, S., Yang, Z., Lin, H., Zhu, J., Liu, L., Wang, W., Liu, S., Liu, W., Ma, Y., Zhang, L., Cao, X., 2018. Self-recognition of an inducible host lncRNA by RIG-I feedback restricts innate immune response. Cell 173, 906–919. e913.

Kato, H., Takeuchi, O., Sato, S., Yoneyama, M., Yamamoto, M., Matsui, K., Uematsu, S., Jung, A., Kawai, T., Ishii, K.J., Yamaguchi, O., Otsu, K., Tsujimura, T., Koh, C.S., Reis E Sousa, C., Matsuura, Y., Fujita, T., Akira, S., 2006. Differential roles of MDA5 and RIG-I helicases in the recognition of RNA viruses. Nature 441, 101–105.

Liu, R., Wu, K., Li, Y., Sun, R., Li, X., 2020. Human antigen R: a potential therapeutic target for liver diseases. Pharmacol. Res. 155, 104684.

Machado, R.S., Gomes-Neto, F., Aguiar-Oliveira, M.L., Burlandy, F.M., Tavares, F.N., da Silva, E.E., Sousa Jr., I.P., 2022. Analysis of Coxsackievirus B5 infections in the central nervous system in Brazil: insights into molecular epidemiology and genetic diversity. Viruses 14, 899.

McNab, F., Mayer-Barber, K., Sher, A., Wack, A., O'garra, A., 2015. Type I interferons in infectious disease. Nat. Rev. Immunol. 15, 87–103.

Ouyang, J., Zhu, X., Chen, Y., Wei, H., Chen, Q., Chi, X., Qi, B., Zhang, L., Zhao, Y., Gao, G.F., Wang, G., Chen, J.L., 2014. NRAV, a long noncoding RNA, modulates antiviral responses through suppression of interferon-stimulated gene transcription. Cell Host Microbe 16, 616–626.

Palomo-Irigoyen, M., Perez-Andres, E., Iruarrizaga-Lejarreta, M., Barreira-Manrique, A., Tamayo-Caro, M., Vila-Vecilla, L., Moreno-Cugnon, L., Beitia, N., Medrano, D., Fernandez-Ramos, D., Lozano, J.J., Okawa, S., Lavin, J.L., Martin-Martin, N., Sutherland, J.D., De Juan, V.G., Gonzalez-Lopez, M., Macias-Camara, N., Mosen-Ansorena, D., Laraba, L., Hanemann, C.O., Ercolano, E., Parkinson, D.B., Schultz, C.W., Arauzo-Bravo, M.J., Ascension, A.M., Gerovska, D., Iribar, H., Izeta, A., Pytel, P., Krastel, P., Provenzani, A., Seneci, P., Carrasco, R.D., Del Sol, A., Martinez-Chantar, M.L., Barrio, R., Serra, E., Lazaro, C., Flanagan, A.M., Gorospe, M., Ratner, N., Aransay, A.M., Carracedo, A., Varela-Rey, M., Woodhoo, A., 2020. HuR/ELAVL1 drives malignant peripheral nerve sheath tumor growth and metastasis. J. Clin. Invest. 130, 3848–3864.

Posnakoglou, L., Tatsi, E.B., Chatzichristou, P., Siahanidou, T., Kanaka-Gantenbein, C., Syriopoulou, V., Michos, A., 2021. Molecular epidemiology of enterovirus in children with central nervous system infections. Viruses 13, 100.

Rothamel, K., Arcos, S., Kim, B., Reasoner, C., Lisy, S., Mukherjee, N., Ascano, M., 2021. ELAVL1 primarily couples mRNA stability with the 3' UTRs of interferon-stimulated genes. Cell Rep. 35, 109178.

Suarez, B., Prats-Mari, L., Unfried, J.P., Fortes, P., 2020. LncRNAs in the type I interferon antiviral response. Int. J. Mol. Sci. 21, 6447.

Sui, B., Chen, D., Liu, W., Wu, Q., Tian, B., Li, Y., Hou, J., Liu, S., Xie, J., Jiang, H., Luo, Z., Lv, L., Huang, F., Li, R., Zhang, C., Tian, Y., Cui, M., Zhou, M., Chen, H., Fu, Z.F., Zhang, Y., Zhao, L., 2020. A novel antiviral lncRNA, EDAL, shields a T309 O-GlcNAcylation site to promote EZH2 lysosomal degradation. Genome Biol. 21, 228.

Teng, P., Yang, H., Li, J., Yang, F., Chen, W., 2022. Analysis of the long noncoding RNA profiles of RD and SH-SY5Y cells infected with coxsackievirus B5, using RNA sequencing. Arch. Virol. 167, 367–376.

Tsuno, K., Miyatake, C., Nishijima, H., Hotta, C., Ogawa, T., Asano, T., 2018. Coxsackievirus B5 aseptic meningitis in infants in Chiba Prefecture, Japan, in 2016. J. Nippon Med. Sch. 85, 187–190.

Wang, J., Wang, Y., Zhou, R., Zhao, J., Zhang, Y., Yi, D., Li, Q., Zhou, J., Guo, F., Liang, C., Li, X., Cen, S., 2018. Host long noncoding RNA lncRNA-PAAN regulates the replication of influenza A virus. Viruses 10, 330.

Wang, K.C., Chang, H.Y., 2011. Molecular mechanisms of long noncoding RNAs. Mol. Cell 43, 904–914.

Wang, Y., Wang, P., Zhang, Y., Xu, J., Li, Z., Li, Z., Zhou, Z., Liu, L., Cao, X., 2020. Decreased expression of the host long-noncoding RNA-GM facilitates viral escape by inhibiting the kinase activity TBK1 via S-glutathionylation. Immunity 53, 1168–1181. e7.

Wu, J., Chen, Z.J., 2014. Innate immune sensing and signaling of cytosolic nucleic acids. Annu. Rev. Immunol. 32, 461–488.

Xu, J., Wang, P., Li, Z., Li, Z., Han, D., Wen, M., Zhao, Q., Zhang, L., Ma, Y., Liu, W., Jiang, M., Zhang, X., Cao, X., 2021. IRF3-binding lncRNA-ISIR strengthens interferon production in viral infection and autoinflammation. Cell Rep. 37, 109926.

Yang, P., Shi, D., Fu, J., Zhang, L., Chen, R., Zheng, B., Wang, X., Xu, S., Zhu, L., Wang, K., 2022. Atomic structures of coxsackievirus B5 provide key information on viral evolution and survival. J. Virol. 96, e0010522.

Yao, Q., Xie, Y., Xu, D., Qu, Z., Wu, J., Zhou, Y., Wei, Y., Xiong, H., Zhang, X.L., 2022. LncEST12, which is negatively regulated by mycobacterial EST12, suppresses antimycobacterial innate immunity through its interaction with FUBP3. Cell. Mol. Immunol. 19, 883–897.

Young, L.E., Sanduja, S., Bemis-Standoli, K., Pena, E.A., Price, R.L., Dixon, D.A., 2009. The mRNA binding proteins HuR and tristetraprolin regulate cyclooxygenase 2 expression during colon carcinogenesis. Gastroenterology 136, 1669–1679.

Yu, X., Li, Y., Ding, Y., Zhang, H., Ding, N., Lu, M., 2020. HuR promotes ovarian cancer cell proliferation by regulating TIMM44 mRNA stability. Cell Biochem. Biophys. 78, 447–453.

Zhang, Y., Cao, X., 2016. Long noncoding RNAs in innate immunity. Cell. Mol. Immunol. 13, 138–147.

Zhao, L., Xia, M., Wang, K., Lai, C., Fan, H., Gu, H., Yang, P., Wang, X., 2020. A long non-coding RNA IVRPIE promotes host antiviral immune responses through regulating interferon beta1 and ISG expression. Front. Microbiol. 11, 260.